

Water Conservation & Management (WCM)

DOI: http://doi.org/10.26480/wcm.03.2025.508.519



ISSN: 2523-5664 (Print) ISSN: 2523-5672 (Online) CODEN: WCMABD

RESEARCH ARTICLE

HARNESSING THE **GREEN METHOD TO SYNTHESIZE COBALT** NANOPARTICLES AND TESTING ITS PERFORMANCE IN TREATING THE HIDDEN POLLUTION OF FLUORIDE FROM AQUEOUS SOLUTIONS

Rasha Salim Mahmooda, Mohammed Nsaif Abbasha, Zaidun Naji Abudia, Alanood A. Alsarayrehc

- ^aEnvironmental Engineering Department, College of Engineering, Mustansiriyah University, Baghdad, Iraq
- bMaterials Engineering Department, College of Engineering, Mustansiriyah University, Baghdad, Iraq
- ^cChemical Engineering Department, College of Engineering, Mutah University, Al Karak, Jordan
- *Corresponding Author Email: mohammed.nsaif.abbas@uomustansiriyah.edu.iq

This is an open access journal distributed under the Creative Commons Attribution License CC BY 4.0, which permits unrestricted use, distribution, and reproduction in any medium, provided the original work is properly cited

ABSTRACT

Article History:

Received 11 April 2025 Revised 21 May 2025 Accepted 17 June 2025 Available online 9 August 2025

Fluoride ion pollution is a problem that needs attention, as it is considered a hidden type of pollution due to its lack of direct or immediate effects. This study aimed to achieve comprehensive environmental treatment by preparing a high-performance adsorbent from non-valuable materials and then using it in the treatment of polluted water. The ability of cobalt oxide nanoparticles (prepared by green method) to treat aqueous solutions contaminated by high fluoride concentrations was investigated, using a batch adsorption unit and under various operating conditions. The obtained results showed that the prepared material was within the nanoscale range with an average size of 271.48 nm, with a surface area of 329 m2/g, possessing multiple functional groups, and a porous structure that qualifies it to be an effective adsorption medium, while its zerocharge point was 7.88. The treatment efficiency varied directly with the nano cobalt oxide dose, contact time, and agitation speed, while it had an inverse relationship with temperature and the fluoride initial concentration. While, the acid function had a dual effect, as the treatment efficiency increased between pH 1-5.5, then began to decrease, reaching the lowest value at pH=9. Nano-cobalt oxide contributed to recover 87%of the contaminated fluoride, with an adsorption capacity of 7.43 mg/g, recorded at 450 rpm, 94 ppm, 5.5, and 1.1 g, for each of the agitation speed, initial fluoride concentration, pH, and nano-cobalt oxide dosage, respectively, after three hours of treatment and at room temperature. The morphological study showed that the prepared nanomaterial suffered from obvious changes represented by the displacement and disappearance of peaks and the appearance of new peaks, a decrease in the surface area by 97%, agglomeration and blockage in the porous structure, dispersion of magnetic particles, increased roughness of the adsorption surface, and modification in the crystallization phases, as indicated by FTIR, BET, AFM, VSM, FESEM, and XRD tests, respectively, which reflects the effectiveness of the preparation method and the efficiency of the nanomaterial as an adsorption medium.

KEYWORDS

Adsorption, batch unit, fluoride ion, mandarin leaves, nano cobalt oxide, removal

1. Introduction

Given the high levels of pollution and the diverse types of pollutants that affect all elements of the environment, providing water suitable for human consumption has become a basic and urgent necessity, especially now, in light of these challenges (Khaleel et al., 2022). Beyond the effects of pollution by heavy metals, pesticides, carcinogenic compounds, plastics, organic materials, pharmaceuticals, eutrophication elements, organic toxic materials, hazardous waste, and others, inorganic pollutants are a particularly important problem, equally significant to the aforementioned pollutants, due to the lack of attention and focus on them, and the primary reason being their hidden nature, as their impact is not immediately apparent (Alsarayreh et al., 2024; Abd Al-Latif et al., 2023; Alwan et al., 2021; Abbas, 2015; Ibrahim et al., 2020a; Alminshid et al., 2025; Abbas and Alalwan, 2019; Hashem et al., 2021; Abd ali et al., 2018; Abbas and Abbas, 2013a). One of the most important pollutants in this category is fluoride, which poses a risk if its concentrations exceed local and global limits and

may lead to fluoride poisoning. Fluoride is known to be a vital component of teeth and contributes to bone formation (Shaji et al., 2024). The highly toxic gaseous element fluorine (F2) is the primary source of the stable, fluoride anion (F-). This ion is found in rocks and soils in varying proportions, as well as in large areas of salt water (Ahmad et al., 2022). Fluoride ion is a component of many compounds, and because it is colorless, it takes on the color of the element to which it is bound. In calcium fluoride and sodium fluoride, it is white, while in combination with nickel, iron, and cobalt, it turns green, brown, or pink. When hydrofluoric acid is formed, it remains colorless (NCBI, 2025). The body needs fluoride ions in limited doses, as it contributes to the composition of bones and tooth enamel in the form of calcium fluoride, which gives them hardness, strength, and increased density. Fluoride enters the human body through various sources, primarily food and drink, which contain small amounts of fluoride. Rice, barley, meat, fish, fruits, vegetables, and some plant products are major sources of fluoride. The amount of fluoride in them is estimated to be between 1-5 mg/kg, while the amount of fluoride in some types of tea and coffee ranges between 0.7-15 mg/kg (Everett, 2011). Just as humans

Access this article online



Website: www.watconman.org DOI:

10.26480/wcm.03.2025.508.519

obtain fluoride through their diet, they also obtain it through toothpastes and mouthwashes containing fluoride. Fluoride contributes to providing essential minerals for teeth and also prevents acid buildup in the mouths of both adults and children, thus promoting dental health (Jaudenes et al., 2020). Consuming fluoride over long periods has no harmful effects, provided that the recommended daily dose is adhered to (NCBI, 2025). However, exceeding the recommended dose may cause some health problems, as increased exposure to fluoride during the first six years of life may lead to what is known as excessive dental fluorosis. In addition, fluoride can cause acute toxicity if a large dose is taken at once (Shaji et al., 2024). This toxicity is accompanied by symptoms such as abdominal pain, diarrhea, vomiting, increased salivation, and thirst. Long-term fluoride toxicity occurs when small amounts of fluoride are consumed through water—such as concentrations above 8 ppm—for long periods. This results in skeletal fluorosis, which is accompanied by a gradual increase in bone density and joint stiffness accompanied by pain (Guth et al., 2020). Fluoride pollution of water occurs from two types of sources. The first source is natural, such as its seepage from the Earth's crust or rocks containing fluoride into groundwater. Human activities, such as industries that use this ion, represent the second and highest source of fluoride pollution (Ahmad et al., 2022). Prominent among these industries are aluminum production, iron and steel production, phosphate fertilizer production, glass and ceramic manufacturing, and pesticide production, in addition to coal burning in power plants. Toothpaste, some medications, and detergents, which are transported into various water sources via sewage, are also a cause of fluoride pollution (Guth et al., 2020). In Iraq, Iraqi Standard No. 417 of 2001 for Drinking Water, specifies that 1 mg/L is the permissible fluoride concentration, which is consistent with the standards in many countries around the world, such as Australia, China, the European Union, and Canada (IQS, 2001). The maximum permissible concentration of fluoride in drinking water is 1.5 mg/L, according to data from the World Health Organization (WHO), while India has set the approved concentration range between 0.6-1.2 mg/L, as documented by the Bureau of Indian Standards (BIS). In the United States, the situation is different. The US Environmental Protection Agency (USEPA) has set the permissible concentration at no more than 4 mg/L, while the Department of Health and Human Services (HHS) has recommended that the concentration not exceed 0.7 mg/L, to reduce the incidence of dental fluorosis and prevent tooth decay (Karunanithi et al., 2023). Given these serious effects and to protect public health, it has become necessary to accurately and continuously monitor fluoride concentrations released into surface and groundwater, as well as to research ways to improve current treatment methods and develop new methods to eliminate the risk of fluoride ion contamination (Ali et al., 2023). Currently, there are many methods used to treat various pollutants in general and high concentrations of fluoride ions in particular, such as chemical precipitation, ion exchange, reverse osmosis, coagulation-flocculation, sedimentation, filtration, ozonation, advanced oxidation process, electrocoagulation, phytoremediation, evaporation, disinfection (SODIS), or biological treatment using appropriate microorganisms (Rajaa et al., 2023). All of the above methods vary in their efficiency, as each has its own conditions and nature. However, they all share one commonality: they all have drawbacks and limitations that make their continued use highly demanding (Al-Ali et al., 2023). Some are expensive, some require initial treatment or ongoing maintenance, others require specialized equipment, large spaces, consume high amounts of energy, are unable to treat pollutants at extreme concentrations, are significantly affected by changing operating conditions, or produce unwanted materials that require additional treatment to dispose of (Abbas et al., 2020). However, adsorption has overcome most of these limitations. It is a simple and inexpensive technology that does not require sophisticated control systems, specialized equipment, or trained personnel (Abbas and Abbas, 2013b). In addition, it is highly efficient in treating various types of pollutants, such as dyes, water hardness, heavy metals, organic acids, mixed pollutants, inorganic toxic, and others, not only from water, but also from crude oil, soil, and air (Abbas and Abbas, 2013c; Abbas et al., 2019a; Ali et al., 2021; Alalwan et al., 2020; Ali and Abbas, 2020; Abbas and Abbas, 2014; Alsarayreh et al., 2025a; Ibrahim et al., 2021; Alalwan et al., 2021). Adsorption is highly efficient in removing contaminants, given that well-known adsorption media such as activated carbon, alumina, high-performance zeolite, and nanomaterials, which possess unique properties, including high surface area, diverse functional groups, and the ability to be reactivated multiple times, making them ideal materials for water purification (Ali et al., 2020a; Alminshid et al., 2021; Khudair et al., 2024; Shadhan et al., 2024; Maddodi et al., 2020). However, this technology faced other drawbacks, including the high cost of producing the adsorption media, the loss of unspecified amounts of their weight with each reactivation process, and the accumulation of these media laden with toxins. This led environmental researchers to search for suitable alternatives for preparing these materials (Abbas and Ibrahim, 2020). One type of alternative is agricultural waste, which possesses characteristics that make it unique in water treatment. It is available yearround, non-toxic, non-value-added, and possesses functional groups suitable for the task of removing pollutants (Abdulkareem et al., 2023). Furthermore, its accumulation causes pollution with dire consequences for the aquatic environment and soil and even to the animals (Abd Ali et al., 2024) (Ali et al., 2024a). The most important types of agricultural waste used in water treatment are rice husks, banana peels, pineapple peels, egg shells, pomegranate peels, orange peels, mandarin peels, tangerine peels, lemon peels, watermelon rinds, wasted tea leaves, water hyacinth, algae, tree leaves, and other types of waste aluminum foil (Ghulam et al., 2020; Alhamd et al., 2024b; Abbas et al., 2019b; Al-Hermizy et al., 2025; Alsarayreh et al., 2025b; Abbas and Nussrat, 2020; Al-Hermizy et al., 2022; Gadooa et al., 2025; Alhamd et al., 2024a; Hasan et al., 2021; Ali et al., 2024b; Alalwan et al., 2021; Ibrahim et al., 2025; Abdullah et al., 2023; Alalwan et al., 2018). To address the problem of toxic waste accumulation after the adsorption treatment process is complete, the concept of zero residue level emerged to dispose of it in a safe and environmentally friendly manner, by considering these residues as raw materials and exploiting them in the preparation of useful materials such as acetone, rodenticide, soil fertilizer, bioethanol, concrete additives, or catalyst and others (Abbas et al., 2021; Abbas et al., 2022a; Hamdi et al., 2024; Abbas, 2015; Ibrahim et al., 2020b; Abbas et al., 2022b; Hammed et al., 2025). This study aimed to achieve a sustainable environmental approach by applying the concept of zero residue level by exploiting the aqueous extract of Iraqi mandarin plant leaves with cobalt nitrate hexahydrate as a precursor to prepare cobalt oxide nanoparticles and to investigate the use of the prepared nanomaterial as an adsorption medium for treating aqueous solutions contaminated with fluoride ions in a batch adsorption system and under different operating conditions. In addition, the morphological changes occurring due to the adsorbent were determined through a number of tests such as FTIR, BET, AFM, VSM, FESEM, and XRD.

2. EXPERIMENTAL ASPECT

2.1 Chemicals

Many chemicals were used to accomplish the objectives of the current study. These chemicals were carefully selected from reputable sources to ensure the accuracy of the results. Cobalt nitrate hexahydrate salt, of Co(NO3)2·6H2O chemical formula and 291.03 g/mol molecular weight, was obtained from Strem Chemicals Inc, USA as a red crystalline powder of \geq 99% purity. While PanReac AppliChem, Spain, supplied sodium fluoride salt of a chemical formula (NaF), molecular weight (41.99 g/mol) and purity (\geq 97%). To provide the acidic medium, 35-38% hydrochloric acid (HCl) solution produced by Thomas Baker, India, was used. To obtain the basic medium, caustic soda (Sodium Hydroxide, Hi-LR^M) of 97.00-103.00% purity was used, which was purchased from HiMedia Laboratories Pvt. Ltd, India in the form of pellets. Double-distilled water with a conductivity of (2.3 μ s/cm at 25 °C) was used to prepare the required solutions, where the laboratory distillation unit GFL-2012, Germany was the source of water used.

2.2 Laboratory equipment used

In the present study, a highly sensitive digital electronic balance (Sartorius BCE3202i-1S, ± 0.01g, Germany) was used to measure the quantities of materials with an accuracy of three orders of magnitude. The plant samples were crushed using a porcelain mortar and pestle (Comet, Diwakar Instruments, India) measuring 4.2" wide and 2.5" tall for mortar and 4.7" in length and the rounded end measures 1.1" for pestle, while the samples were ground and dried using laboratory equipment (Mortar Grinder RM 200-Retsch, Germany) and (Laboratory Drying Oven-99200-3, Stanhope-Seta, UK), respectively. To determine acidity and basicity, use a digital device (Sartorius PB-10, ± 0.01, Germany) capable of measuring hydrogen ion concentration in the range of (0-14) pH units. The magnetic stirrer hot plate was of the type (MI0102003, FOUR E'S SCIENTIFIC, China), while to purify the required plant extract, a centrifuge of the type (HERMLE Labortechnik GmbH, Z 206 A, Germany) was used. The Thermo Scientific MaxQ™ 7000 SHKE7000 was the most prominent piece of equipment used to conduct all experiments to test the performance of cobalt oxide nanoparticles as an adsorbent for fluoride ions. The aqueous solutions resulting from the adsorption treatment process were analyzed using a double-beam UV/Vis spectrophotometer (Analytik Jena AG-3715013, Germany), after filtering the samples using qualitative Whatman filter paper no.1 (GE Whatman 1001-6508, 10 mm diameter) and then by a vacuum filtration kit (EIS-CH200501- CP LabSafety, USA). Finally, the glassware of all sizes and types used to complete the study were of borosilicate glass, supplied by (Adarsh Scientific Industries, India), while the 500 ml amber glass jar of black plastic lid was supplied by (Ampulla

LTD, UK).

2.3 Collection and preparation of mandarin plant leaves

Fresh leaves of the Iraqi mandarin plant, used as the primary precursor in the preparation of nanoparticles, were collected from local markets in the capital, Baghdad, during the period from October 1, 2024, to November 30, 2024, and were identified as leaves of the Iraqi mandarin plant after taxonomic confirmation at the herbarium of the Biology Department, College of Education for Pure Sciences, University of Diyala. The identified leaves were first thoroughly washed with tap water until completely free of impurities, dust, and dirt.



Figure 1a: Iraqi mandarin leaves



Figure 1b: Iraqi mandarin leaves powder

They were then washed with double-distilled water, as this type of water has the ability to remove any contaminants that are still attached. The washed leaves were dried in two steps. Firstly, they were exposed to the open air in a clean place away from dust for a period of 3 winter days, at a rate of 10 hours per day. The subsequent drying step was completed using an electric oven at 50°C , to ensure that the leaf structure did not change or crack. The drying process continued until the weight was stable. The mandarin leaves were then manually torn into as small pieces as possible. The torn leaves were then ground using a mortar and pestle, before being ground in a laboratory grinder to produce a fine, homogeneous powder. Finally, the Iraqi mandarin leaves powder was stored in an amber glass jar covered with aluminum foil layer in a clean, dry place until subsequent use. Figure 1 shows the Iraqi mandarin leaves plant used.

2.4 Preparation of Nanoparticles

The cobalt oxide nanoparticle preparation process involved three basic steps, according to the method described by (Hameed and Abbas, 2024). The first step was the preparation of the aqueous plant extract of Iraqi mandarin leaves, which served as the primary precursor. The second precursor, a mineral solution of cobalt nitrate, was the next step in the process. The final step was conducting the green reaction between the aforementioned two precursors under operating conditions favorable for the synthesis of cobalt oxide nanoparticles.

2.5 Preparation of plant aqueous extract

Using 150 ml glass flask closed by stopper, and covered by a layer of aluminum foil, 12 g of Iraqi mandarin leaves powder was soaked in 1 liter of double-distilled water for 15 minutes, then the mixture was heated using a magnetic stirrer hot plate for 120 minutes at 150 rpm and $60^{\circ}\text{C}.$ The mixture was allowed to cool to room temperature and then filtered using Whatman filter paper twice. The mixture was then centrifuged at 5,000 rpm to ensure the purity of the extract from impurities and suspended particles. The final extract was stored in a refrigerator at 4°C until used as a precursor to prepare cobalt oxide nanoparticles.

2.6 Preparation of mineral solution

The mineral solution is the main precursor of nanoparticles, as it represents the indispensable metal source in those particles. To obtain cobalt oxide nanoparticles, cobalt nitrate hexahydrate was chosen as the main source of cobalt ions due to its high solubility in water (38.3 g/100 g water at 25 °C), the lack of effect of nitrate ions on other components of the plant solution, and the ease of getting rid of nitrate after achieving the reaction between the two precursors. To prepare a solution of 0.02 M cobalt nitrate, $6.00\,\mathrm{g}$ of cobalt nitrate powder were dissolved in a specified volume of double-distilled water in a glass beaker using a magnetic stirrer at 150 rpm at room temperature. Stirring is continued until the cobalt nitrate powder is completely dissolved. The entire solution is then carefully transferred to a 1,000 cm3 volumetric flask using a suitable glass funnel before making up to 1 liter with double-distilled water. The volumetric flask is covered by a layer of aluminum foil, and the metal solution is stored in a clean, dry, and dark place, away from sunlight to prevent any potential influence of light or weather conditions.

2.7 Green reaction

Before conducting the reaction between the precursors, the aqueous extract of plant is prepared by leaving it in a clean place at room temperature overnight. After the temperature of the aqueous extract of Iraqi mandarin leaves has equalized with the laboratory temperature, 20 ml of it is mixed with 100 ml of the other precursor, a cobalt nitrate solution, at a volume ratio of 1/5. The green reaction between the precursor occurs by slowly adding the required volume of the plant aqueous extract to the corresponding volume of the mineral solution in a 150 ml glass beaker. The preparation process of nanoparticle is carried out by continuously stirring the contents of the glass beaker using a magnetic stirrer hot plate to achieve a homogeneous distribution of ions and prevent particle agglomeration during the reaction. The mixing process of the precursor mixture continued for 180 minutes at 85°C and 150 rpm to stabilize the synthesized cobalt oxide nanoparticles by inducing the plant compounds in the aqueous extract to reduce cobalt ions and evaporate water from the solution. Continuous heating facilitates the self-combustion of the precursor mixture components and vaporization of organic materials, thus producing a bold slurry containing the synthesized cobalt oxide nanoparticles. The resulting slurry is left to reach ambient temperature, after which it is centrifuged at 10,000 rpm to separate the solid particles from the remaining solution (supernatant), before being washed three times with deionized water to remove any suspended impurities. The washed powder was dried in an electric furnace at boiling point until the weight was constant, before being annealed for 120 minutes at 400°C to achieve structural stability and achieve a crystalline state. The prepared cobalt oxide (Co304) nanoparticles were stored in an amber jar until their performance as an adsorbent for fluoride ions was tested.

2.8 Point of zero charge (pHpzc)

The point of zero charge is determined by testing the effect of synthesized cobalt oxide nanoparticles on the pH difference of aqueous solutions prepared at different pH values. To accurately determine the point of zero charge of the target substance, the pH values of aqueous solutions are adjusted to include acidic, neutral, and basic pH behavior using preprepared hydrochloric acid and sodium hydroxide solutions. Within the range of 1-14, the point of zero charge of cobalt oxide nanoparticles, prepared from the aqueous extract of the leaves of Iraqi mandarin plant and a cobalt nitrate solution as a precursor, was studied by measuring the difference in pH of the aqueous solution before and after adding a specific weight of the nanoparticle. The point of zero charge was determined by plotting the data of pH and $\Delta \rm pH$, and the pHpzc is the value of pH at zero.

2.9 Stock solution of fluoride anions

The stock solution provides the primary source of fluoride ions in the current study. Aqueous solutions with the required concentrations of fluoride ions can be prepared using dilution, without the need to repeat the preparation process. This significantly reduces the error in measuring fluoride ions after adsorption. Sodium fluoride salt (NaF) is used as a source of fluoride anions, due to its moderate solubility in water (42 g/L at $20~^\circ\text{C}$) and its low toxicity compared to other compounds of fluoride such as hydrofluoric acid. At room temperature, in an appropriate amount of double-distilled water, 1.11 g of sodium fluoride was dissolved in a suitable sized glass beaker, stirring continuously with a glass rod until the entire amount is dissolved. Carefully transfer the solution to a volumetric flask using a glass funnel, and then make up to 500 ml with double-distilled water. Each ml of the resulting solution contains 1 ppm of fluoride anion, depending on the molecular weight of the salt used and the target ion.

2.10 Adsorption Unit

In a batch adsorption unit, the performance of cobalt oxide nanoparticles, prepared from the extract of Iraqi mandarin leaves and cobalt nitrate solution as precursor, as an experimental adsorption medium for the removal of fluoride ions from contaminated aqueous solutions was investigated. Simulated solutions of different concentrations of fluoride anion were prepared by diluting. Using double-distilled water, certain volumes of the previously prepared stock solution, and the pH of each solution was adjusted using 1M solutions of both sodium hydroxide and hydrochloric acid. Then, the specified amount of adsorbent is added to each sample and their numbers are recorded. The experimental flasks, covered with a layer of aluminum foil and tightly tied with a rubber band, are charged into the water bath shaker. After adjusting the agitation speed and the temperature of the batch unit to the required values, the adsorption process begins and continues until the required time period was ended, at which point the adsorption unit stops automatically. Each experiment was conducted with 3-5 replicates, with each experiment involving feeding 100 ml of the contaminated solution into 150 ml glass beakers, to ensure free movement of the solution during shaking. The operating conditions studied in the current investigation covered the widest ranges reported in the literature to accurately determine the adsorption behavior of the prepared nanomaterials. The parameters studied ranged from 3-9 for the pH parameter, 100-500 rpm for the agitation speed, 1-100 ppm for the initial concentration of fluoride anion, and 0.05-1.2 g of nano-cobalt oxide. The effect of contact time was studied in the range of 10-200 min, and the effect of temperature was studied in the range of 25-50 °C. After the specified time has elapsed, the experimental flasks are carefully extracted and filtered, first using filter paper and then using a vacuum filtration kit to extract the entire mass of the prepared cobalt oxide nanoparticle. The absence of adsorbent in the treated aqueous solution ensures the accuracy of the calculated fluoride anion concentration after adsorption. The samples were tested after adsorption using a UV/Vis spectrophotometer and a SPADNS detector, and the absorbance readings corresponding to each sample were recorded. According to the calibration curve, the concentration fluoride anion in the adsorption sample was determined. Thus, the percentage removal efficiency and adsorption capacity were calculated using equations (1) and (2), respectively:

$$\%R = \frac{c_{in} - c_{out}}{c_{in}} \times 100 \tag{1}$$

$$q = \frac{v}{w} (C_{in} - C_{out}) \tag{2}$$

Where: %R represents the percentage removal efficiency of fluoride anion from the sample (%), C_{in} and C_{out} represent the concentration of fluoride anion in the solution before and after adsorption by cobalt oxide nanoparticle, respectively (ppm), q: adsorption capacity of the adsorbent (mg/g), w: mass of cobalt oxide nanoparticle used in the experiment (g), V: volume of the aqueous solution contaminated with fluoride anions used in the experiment (L).

2.11 Calibration curve of fluoride anions preparation

There are several methods for measuring fluoride ion concentrations in aqueous solutions, some traditional and some modern, each with its own advantages and disadvantages. The selection of an appropriate method depends on several factors, including the concentration to be measured and the availability of the necessary materials and equipment. Fluoride concentration measurement methods include sodium hydroxide titration, electrochemical analysis, FTIR spectroscopy, ion-selective electrode (ISE), and colorimetric analysis using SPADNS solution. The latter method is used to determine the fluoride anion values in aqueous solutions after treatment, due to its simplicity and accuracy, especially at very low concentrations of fluoride anions. This method involves the formation of a complex resulting from the reaction of the fluoride anion with one of the zirconium compounds. This resulting complex leads to a change in the color of the solution, which enables the spectrophotometer to measure the difference in absorbance at a wavelength of 570 nm, and thus determine the concentration of the fluoride ion in the solution. According to the colorimetric method, a standard concentration of SPADNS (sodium 2-(parasulfophenylazo)-1,8-dihydroxynaphthalene-3,6-disulfonate) prepared by dissolving a specific amount of the substance in a known volume of distilled water as a first step. In the next step, a zirconium solution is prepared by dissolving zirconium chloride in distilled water. By mixing the two solutions in precise and specific proportions, the reagent required to determine the fluoride ion concentration is prepared. It is noted that the relationship is inverse between the absorbance and the concentration of the fluoride anion in the calibration curve performed, where increasing the fluoride concentration leads to a decrease in the color intensity of the detector as a result of the competition between the two (fluoride and the detector), which leads to its liberation from binding with the zirconium ions. Thus, the color of the indicator begins to fade as the concentration increases, indicating that the colorless solution has the highest possible concentration of fluoride anions. Figure 2 shows the calibration curve for fluoride anions prepared in this study, using colorimetric analysis using SPADNS solution.

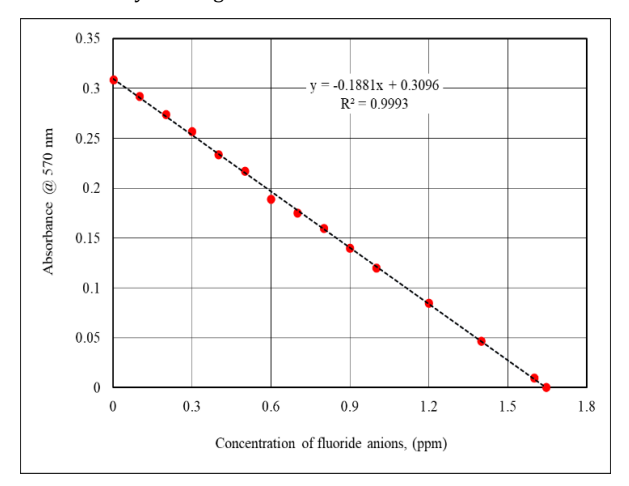


Figure 2: The calibration curve for fluoride anions (F^-) prepared colorimetric method

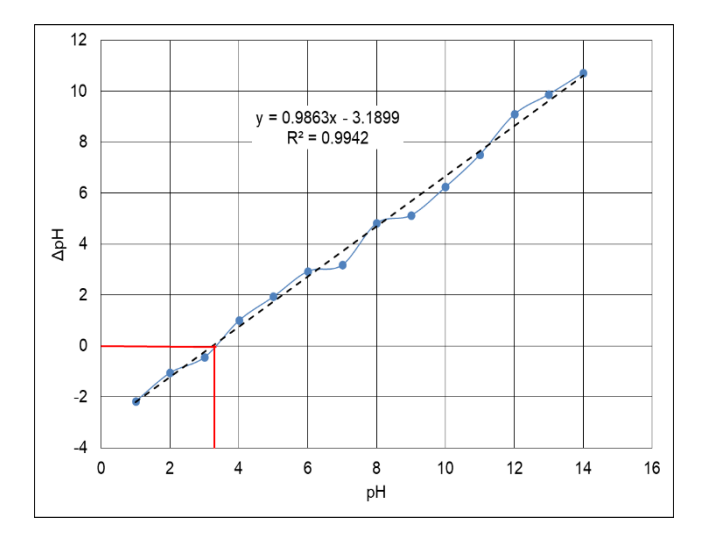


Figure 3: Point of zero charge (pH_{pzc}) of prepared cobalt oxide nanoparticles

3. RESULTS AND DISCUSSION

3.1 Point of zero charge (pH_{pzc})

Figure 3 shows the results obtained from changing the pH values of aqueous solutions corresponding to the surface charge distribution of the adsorbent, at acidic, basic and neutral pH values. It is noted that the surface charge of cobalt oxide nanoparticles is more negative at low pH values, specifically between 1-7, which confirms that the nanomaterial contains active groups that have the ability to capture positive hydrogen ions and bind with them, making the surface negatively charged and highly protonated. This means that the prepared cobalt oxide nanoparticles have the ability to adsorb positive ions more efficiently than negative ions within this range. As the pH increases and moves towards neutrality, the negative charge gradually decreases until reaching a pH value of 7.88, at which $\Delta pH = 0$, where the cobalt oxide nanoparticles are chargeless or electrically neutral. After the pH value exceeds 8, the positive charge begins to increase significantly, and its value increases with the increase in the pH value of the solution, as a result of the direct relationship between the two factors. Here, favorable conditions are available for the action of acidic functional groups dispersed on the surface of the nanocobalt oxide (originally protonated), and the nanomaterial begins to capture negative ions more efficiently than in previous conditions. Above pH values greater than 10, the positive charge stabilizes, resulting from surface saturation. Therefore, based on the obtained point of zero-charge value, the effective pH range for removing fluoride anions using the

prepared cobalt oxide nanoparticles should be between 3 and 9, as the adsorbent is ineffective at other ranges.

3.2 Dynamic light scattering (DLS)

Dynamic light scattering analysis of cobalt oxide nanoparticles, prepared from the plant leave extract of Iraqi mandarin and cobalt nitrate hexahydrate solution, was performed using a device (VASCO $\text{KIN}^{\tiny{\text{TM}}}$ Cordouan Technologies, France) operate by NanoQ V2.5.9.0 program. Figure 4 shows the dynamic light scattering (DLS) analysis of cobalt oxide nanoparticles prepared from the aqueous extract of Iraqi mandarin plant leaves and cobalt nitrate hexahydrate solution as precursor. According to the Figure above, it is observed that the prepared nanoparticles are distributed asymmetrically, with multiple peaks emerging, indicating the diversity of size classes in the tested sample. The largest distribution is confined between 100 and 1000 nm, represented by two narrow main peaks at 271.48 nm and 472.82 nm, with the presence of small individual particles due to the aggregation of secondary particles or the occurrence of slight clusters resulting from the effect of hydrogen bonds or van der Waals forces. This result is attributed to the fact that the preparation process resulted in a mixture of varying sizes and no homogeneous distribution of the resulting particles. Although heterogeneity is known in nanomaterial preparation processes, this possibility is excluded because the distribution of the resulting particles is confined between two peaks and no more. The most likely possibility is that the tested sample contains particles with a homogeneous distribution that represents the first peak, while the clumping between a ratio of these particles led to the appearance of the second peak. What confirms this hypothesis is that the height of the first peak is less than the second, while its base is more extended compared to the other peak. It is also noted that the two peaks have a narrow distribution, which confirms the efficient control of the operating conditions of the synthesized nanoparticles.

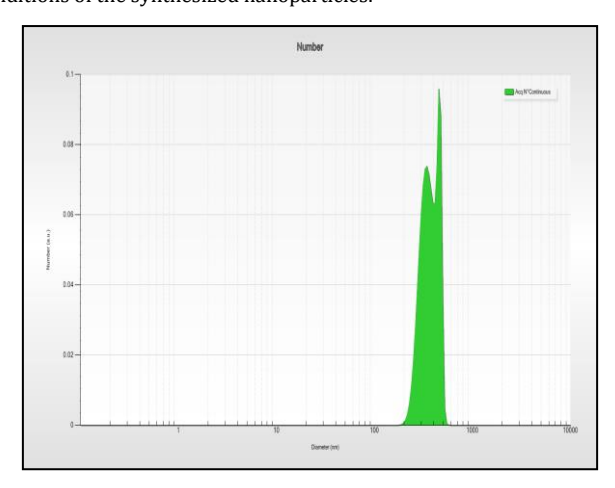


Figure 4: Dynamic light scattering (DLS) analysis of prepared cobalt oxide nanoparticles

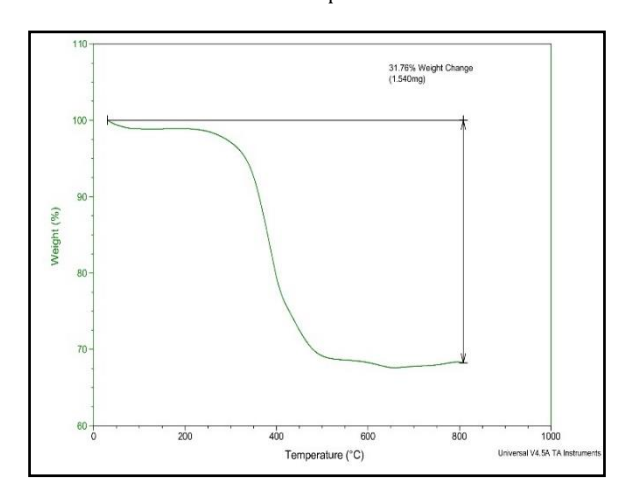


Figure 5: Thermogravimetric Analysis (TGA) examination of prepared cobalt oxide nanoparticles

3.3 Thermogravimetric Analysis (TGA)

Thermogravimetric analysis of cobalt oxide nanoparticles, prepared from extract of Iraqi mandarin leaves and cobalt nitrate hexahydrate solution, was performed using a (TA Instruments SDT Q600 Simultaneous DSC-

TGA, USA) device, as shown in Figure 5. To investigate the thermogravimetric analysis (TGA) of the prepared material, a 4.85 mg sample of cobalt oxide nanoparticles was tested by gradually heating it from room temperature to 1073.15 K, at a rate of 20°C/min, in an inert atmosphere in the presence of argon gas. The analysis revealed a weight loss of 1.54 mg from the original weight. This indicates that the sample contains volatile compounds or organic materials, as well as the possibility of moisture being physically or chemically bound to it. The decrease in sample weight by approximately 31.7% can be explained by the fact that the lost weight represents the decomposition of crystal water or evaporation of moisture, the decomposition of unknown thermally unstable compounds, or the decomposition of organic compounds that were not reduced during the preparation process and are sourced from the aqueous extract of Iraqi mandarin leaves plant. This assumption is supported by the fact that the process takes place in the presence of argon gas, which prevents combustion. Beyond 873.15 K, the curve remains nearly constant, indicating thermally stable inorganic materials, represented by the stable cobalt oxide nanostructure. This result indicates the thermal stability of the prepared material and its organic content compared to the remaining inorganic structure.

3.4 BET Surface area

The surface area of cobalt oxide nanoparticles prepared from Iraqi mandarin leaves extract and cobalt nitrate hexahydrate solution, before and after adsorption of fluoride anions, was investigated using a Qsurf 9600 Thermo Finnegan Co./USA device. Figure 6 shows the adsorption-desorption isotherm curve of the tested cobalt oxide nanoparticles, before adsorption (blue) and after adsorption (red). It is noted from the Figure aformentioned that the virgin adsorbent has a surface area of 329 m²/g. The reason for this high value is due to the nature of nanomaterials, which are characterized by their high surface area, which confirms the success of preparing cobalt oxide particles at the nanoscale. After treatment with solutions contaminated with fluoride anions, the surface area of the adsorbent decreased to less than $10 \, \text{m}^2/\text{g}$, meaning that adsorption consumed approximately 97% of the total surface area.

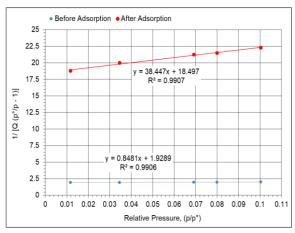


Figure 6: The adsorption-desorption isotherm curve of the prepared cobalt oxide nanoparticles, before adsorption (blue) and after adsorption (red)

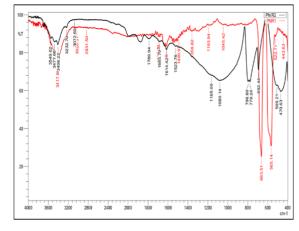


Figure 7: The FTIR curves of the prepared cobalt oxide nanoparticles, before adsorption (red) and after adsorption (black)

This significant decrease is attributed to the ability of cobalt oxide

nanoparticles to adsorb fluoride anions onto their surfaces, due to their highly porous structure and diverse functional groups that contribute to the efficient continuation of the adsorption process. In addition, the prepared nanoparticles are sure to be rich in micropores (≤ 2 nm) and mesopores (2-50 nm), which are pores with high performance in adsorption processes. It is possible that the adsorbed fluoride anions had accumulated in a layer on the surface of the adsorption medium, preventing the nitrogen gas –used in the BET analysis– from reaching all surface pores. Therefore, all explanations share one common result: the prepared cobalt oxide nanoparticles exhibited high performance and contributed to the adsorption of fluoride anions with an efficiency exceeding 87% of their concentration in the contaminated aqueous solution.

3.5 Fourier transform infrared spectroscopy (FTIR)

Fourier transform infrared (FTIR) investigation of cobalt oxide nanoparticles prepared from aqueous extract of Iraqi mandarin leaves and cobalt nitrate hexahydrate solution as precursor, before and after adsorption of fluoride ions, was carried out using an IR Prestige-21, Shimadzu, Japan. Figure 7 shows the FTIR curves of the tested cobalt oxide nanoparticles, before adsorption (red) and after adsorption (black), respectively. Significant peaks in various bands indicate interactions that took place when the cobalt oxide nanoparticles were adsorbed with fluoride anions. The stretching vibrations of the hydroxyl group (OH^-) are responsible for the broad peaks observed at 3549, 3477, 3417, and 3408 cm⁻¹. This suggests the presence of hydrogen bonds and functional groups that can interact with fluoride anions. These groups are involved in the adsorption process because a small change in the strength of these peaks is seen after adsorption. The C-H stretching vibrations in the hydrocarbon groups are responsible for the absorption bands observed at 3232, 3072, and 3020 cm⁻¹. After adsorption, the intensity of these bands decreases significantly, suggesting the presence of surface interactions or the attachment of fluoride anions (F^{-}) to the hydrocarbon group. A small change in the peak at 2831 cm⁻¹ following adsorption suggests that the alkane groups C-H stretches may have a moderate interaction with fluoride anions. At 1789, 1685, and 1614 cm⁻¹, absorption peaks are observed, which correspond to vibrations of the (C=O) group of carbonyl groups or amide bonds. After adsorption, these peaks shift significantly in intensity, suggesting that cobalt oxide nanoparticles may establish bonds with the fluoride anions adsorbed on their surface. The carbon double bond (C=C) vibration peak at 1523 cm-1 in aromatic compounds was unaffected by adsorption, suggesting that the substance's aromatic structure remained mostly unchanged. The presence of fluoride ions and their active involvement in the adsorption process are shown by the change in the peak at 1490 cm⁻¹, which is present in cobalt oxide nanoparticles prior to adsorption but no longer exists after adsorption. The peaks observed in the 1193, 1165, 1108, and 1045 cm⁻¹ wavelength ranges can be attributed to the structural vibrations of the carbonyl groups bonded to oxygen (C-O) and nitrogen (C-N). These groups exhibited clear shifts in position and density following adsorption, confirming their role in the direct binding of fluoride anions. The peaks at wavelengths 796,779, and 692 cm⁻¹ are related to the torsional vibrations of the alkane and inorganic groups, while the peaks at wavelengths 663 and 565 cm⁻¹ are due to the vibrations of ionic bonds with oxygen, indicating the formation of new bonds between the cobalt oxide nanoparticles and the fluoride ions adsorbed on their surfaces. The peaks at 522, 509, and 470 cm⁻¹, which are associated with the structural vibrations of the ionic materials, underwent clear modifications upon adsorption, suggesting that the fluoride anions adsorbed onto the surface of the produced nanomaterial remained stable.

3.6 Atomic Force Microscopy (AFM)

Atomic force microscopy (AFM) test of cobalt oxide nanoparticles prepared from the extract of Iraqi mandarin plant leaves and cobalt nitrate hexahydrate solution as precursor, before and after adsorption of fluoride anions, was performed using a Bruker Dimension XR SPM, USA. Figure 8a and Figure 8b illustrate the AFM images of the tested cobalt oxide nanoparticles, before and after adsorption, respectively. Figure 8a shows that the prepared nanomaterial has a relatively uniform distribution of particles with a homogeneous surface, almost free of large and foreign agglomerates, which confirms the success of the particle synthesis process. In addition, the clear porous structure contributes significantly to the ability of the cobalt oxide nanoparticles to adsorb ions from

contaminated solutions. As for Figure 8b, the material appears in a different state from the virgin particles before adsorption, where an increase in surface roughness and different heights is observed, in addition to the appearance of larger clusters of cobalt oxide nanoparticles as a result of treatment with solutions contaminated with fluoride anions. These changes indicate that the adsorption is of the chemical type resulting from the formation of covalent bonds between the fluoride anions and the active groups on the surface of the adsorbent.

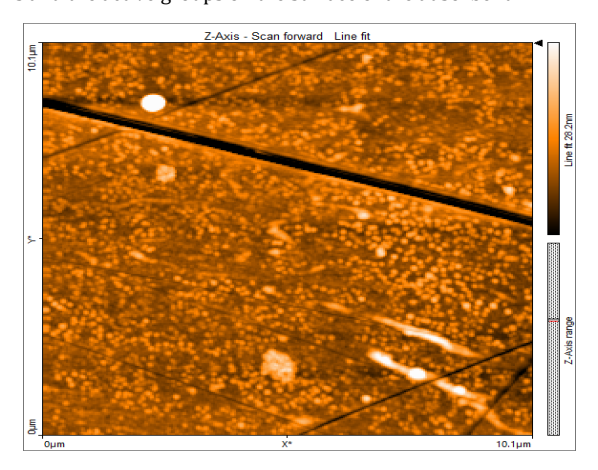


Figure 8a: Atomic Force Microscopy (AFM) image of the prepared cobalt oxide nanoparticles before adsorption

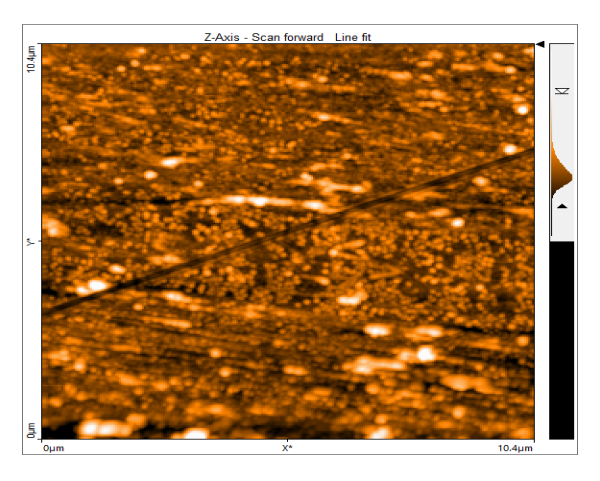


Figure 8b: Atomic Force Microscopy (AFM) image of the prepared cobalt oxide nanoparticles after adsorption

It is also noticeable that the surface porosity of the nanomaterial decreased and that larger aggregates were formed compared to before adsorption. This is attributed to the accumulation of adsorbed anions on the surface, which indicates that the active groups were largely consumed, and that the adsorbed fluoride anions contributed to the formation of surface complexes that altered the surface topography of the cobalt oxide nanoparticles. The results of the atomic force microscopy (AFM) test confirm the efficiency of using the prepared cobalt oxide nanoparticle as an effective adsorption medium for recovering fluoride anions from contaminated solutions.

3.7 Field emission scanning electron microscopy (FESEM)

FE-SEM examination of cobalt oxide nanoparticles prepared from the aqueous extract of Iraqi mandarin leaves and cobalt nitrate hexahydrate solution as precursor, before and after adsorption of fluoride anions, was performed using an SUT-FESEM, MIRA3, TESCAN, Czech Republic. Figure 9a and Figure 9b show the FE-SEM images of the tested cobalt oxide nanoparticles, before and after adsorption, respectively. The particles in Figure 9a, which depicts the virgin cobalt oxide nanoparticles prepared, have a relatively uniform distribution and an average size of approximately 38.67 nm. This suggests that the particles were wellprepared at the nanoscale, with a high surface area, a crucial attribute for efficient adsorption processes. The surface of nanoparticles appears more transparent and has a nanoscale appearance, which indicates that there are active sites on the surface that are prepared to interact with fluoride anions (F^{-}) . As for Figure 9b, which represents the cobalt oxide nanoparticles after adsorption, it is noted that the average particle size has increased to 51.33 nm, which indicates the effect of the adsorption process on the prepared nanomaterial.

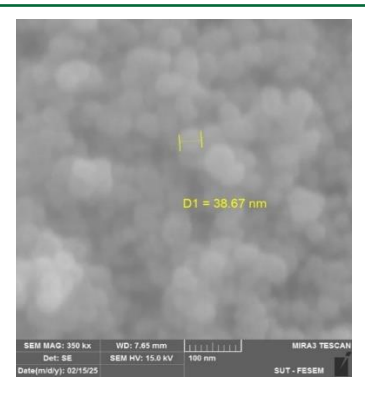


Figure 9a: FE-SEM image of prepared cobalt oxide nanoparticles before adsorption

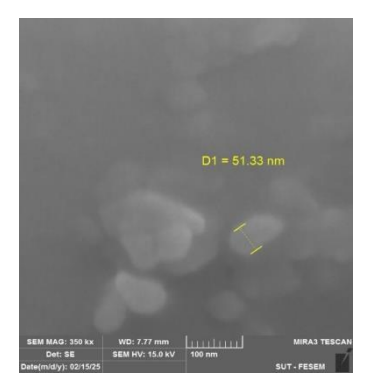


Figure 9b: FE-SEM image of prepared cobalt oxide nanoparticles after adsorption

This increase in the size of the adsorption medium particles can be explained due to the accumulation of fluoride anions over the surface of the cobalt oxide nanoparticles, which causes the nanomaterial's apparent diameter to increase due to the buildup of adsorbed ions. Moreover, changes in the surface nature can be observed between Figure 9a and Figure 9b, as the surface after adsorption became rougher and less clear at the nanoscale level, indicating the formation of a layer of adsorbed fluoride ions that almost completely covered the active sites, which reduced the clarity of the boundaries between the particles.

3.8 Vibrating sample magnetometer (VSM)

VSM test of cobalt oxide nanoparticles prepared from the aqueous extract of Iraqi mandarin leaves and cobalt nitrate hexahydrate solution as precursor, before and after adsorption of fluoride anions, was carried out using an X7404-S 7400 Series VSM, Lake Shore Cryotronics USA. Figure 10 shows the VSM curves of the tested cobalt oxide nanoparticles, before adsorption (blue) and after adsorption (red), respectively. It is noted from the two curves that the cobalt oxide nanoparticles before adsorption have a higher magnetic response than the same material after adsorption. These changes can be explained by several physical and chemical factors, including that the adsorption of fluoride anions (F^{-}) leads to covering the active sites on the surface of the material, which hinders its interaction with the external magnetic field, and thus reduces its magnetic response. Also, interference with the electronic structure resulting from the formation of new bonds between the surface of the cobalt oxide nanoparticles and the adsorbed fluoride ions affects the movement of electrons responsible for the magnetic properties, causing a decrease in the magnetic polarization. Adsorption can reduce the overall magnetic impact of the generated cobalt oxide nanoparticles if non-magnetic fluoride anions (F^{-}) replace active magnetic atoms, the intensity of which is dependent on the type of the adsorbed element. Furthermore, alterations to the crystal structure and distribution of magnetic particles can occur during adsorption. This dispersal of magnetic particles within the material makes them less effective at interacting with external magnetic fields, as they become more spaced out or irregularly distributed after the adsorption process. This effect is also seen in magnetic hysteresis, where the adsorption curve becomes flatter and narrower as it moves past the origin point.

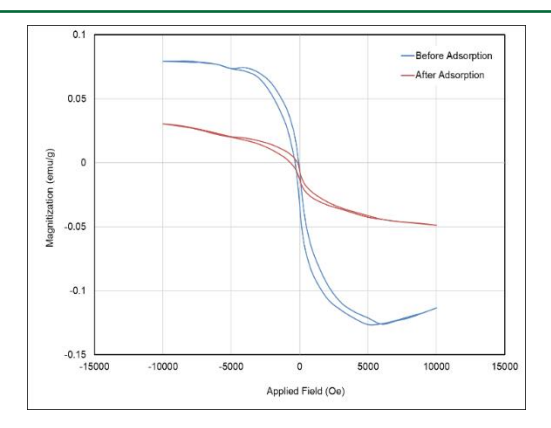


Figure 10: Vibrating sample magnetometer (VSM) curves of prepared cobalt oxide nanoparticles before adsorption (blue) and after adsorption (red)

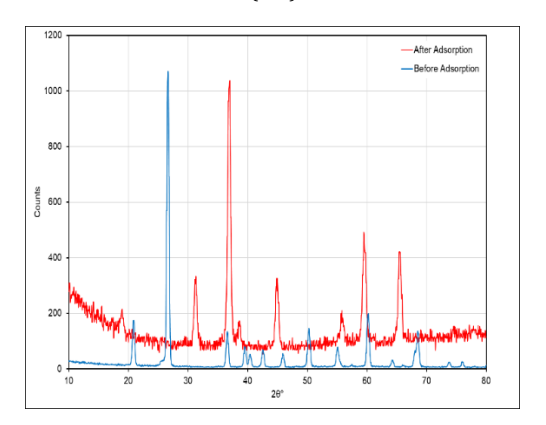


Figure 11: X-ray diffraction (XRD) curves of prepared cobalt oxide nanoparticles before adsorption (blue) and after adsorption (red)

This suggests that the cobalt oxide nanoparticles aren't as good at retaining magnetization once the field is gone, which could be because the adsorbed fluoride ions have an inhibitory effect. Additionally, the overall magnetization may be diminished due to an increase in magnetic dispersion inside the material caused by adsorption, which in turn reduces the influence of local fields that help polarization. As part of the adsorption process, the material's active magnetic centers may undergo changes in oxidation state; thus, the material may become less responsive to external magnetic fields.

3.9 X-ray diffraction

XRD investigation of cobalt oxide nanoparticles prepared from the aqueous extract of Iraqi mandarin leaves and cobalt nitrate hexahydrate solution as precursor, before and after adsorption of fluoride anions, was carried out using an XRD-6100-Shimadzu, Japan, Figure 11 shows the XRD curves of the tested cobalt oxide nanoparticles, before adsorption (blue) and after adsorption (red), respectively. Fluoride anion adsorption altered the crystal structure of the produced cobalt oxide nanoparticles, as seen in Figure 11. Prior to being exposed to polluted solutions, the nanomaterial exhibited distinct and intense basic peaks at 2θ values of 31.33°, 36.14°, 42.72°, 56.89°, and 63.05°, suggesting a highly crystallinity level and a regular crystal structure. The reliability of the nanoscale preparation method is confirmed when these peaks are compared to data from (ICPDS#42-1467), which stands for cobalt oxide Co₃O₄. It is noted that the cobalt oxide nanoparticles in its original state have a high crystallinity and a regular structure, but after treatment with fluoride solutions, a significant decrease in the intensity of the peaks is evident, particularly at 31°, 33°, 36.14°, and 42.72°. This indicating that adsorption has weakened the crystalline order as a result of the adsorbed ions entering the crystal structure after binding to the surface. A slight shift in the peaks, ranging from 0.25 to 0.60, towards smaller angles can also be observed, which may indicate expansion of the crystal lattice due to the entry of ions with larger radii, or a rearrangement of the atoms within the lattice as a result of the adsorption of fluoride ions. Some peaks at values 56.89° and 63.05° of 2θ , also became less distinct or disappeared completely, indicating the formation of new phases or the transformation of the material into a less crystalline or amorphous phase. At 24.85°, 51.02°, and 29.66° of 2θ, new peaks are observed following the adsorption of fluoride anions (F^{-}) . The presence of fluoride anions (F^{-}) due to adsorption and cobalt oxide nanoparticles may have caused a chemical reaction, which might have led to the creation of new molecules. In other words, the adsorption process

involved chemical reactions that resulted in the creation of novel molecules, in addition to physical ones.

4. BEHAVIOR OF THE VARIABLES OF THE ADSORPTION PROCESS OF FLUORIDE ANIONS

This section discusses the effect of varying operational variables within specified ranges on the efficiency of fluoride anions (F^-) removal from contaminated solutions in a batch-mode adsorption unit. Although the operational parameters are interrelated, some are specific to the contaminated solution, others to the adsorbent, and a third to the adsorption unit. As previously mentioned, the design parameters studied are acidity, initial fluoride ion (F^-) concentration, cobalt oxide nanoparticle dosage, agitation speed, contact time, and temperature.

4.1 Effect of pH change on the fluoride anions recover efficiency

The pH is one of the most important operational conditions in any adsorption process, as it affects both the adsorbent and adsorbate simultaneously. Therefore, determining the optimal value of this variable is a priority in any treatment study. Based on the point of zero charge (pH_{pzc}) results, the effect of this factor on the recovery efficiency of fluoride anions (F^{-}) was studied within a range of 3-9, keeping other operators fixed at 300 rpm, 1 ppm, 0.1 g, 180 min, and 25 °C for the agitation speed, initial concentration of fluoride anions (F^-) , dose of cobalt oxide nanoparticles, contact time, and temperature, respectively. Figure 12 shows that the acid function has a dual effect on the ability to remove fluoride anions (F^{-}) , as the relationship between the two variables is initially direct, and the removal increases from 7.62% at pH=3 until it reaches its maximum value of 29.5% at 5.5. Then the relationship turns inverse, as the efficiency decreases until it reaches the lowest value of 3% at pH=9. Low values of pH mean an increase in the concentration of positive hydrogen ions (H^+) in the solution. This leads to protonation of the adsorption surface and its positive charge, which leads to the attraction of fluoride anions (F^{-}) to the surface of the adsorbent, thus increasing the adsorption efficiency. Although increasing the pH value means decreasing the positive charge, the treatment efficiency increases by approximately four times its value. This can be explained by the fact that the ability to form hydrofluoric acid (HF) in the solution decreased due to the increase of hydroxide anions (OH^-) , while the surface of the nanomaterial retained its positive charge, and the adsorption process gradually became dominant over the removal process until reaching the maximum value at a pH of 5.5. Completing the last explanation, the increase in the pH value after 5.5 indicates that the solution moves towards a basic environment, as the concentration of hydroxide ions will gradually increase, leading to competition from negative fluoride ions for the functional groups in the active sites spread on the surface of the adsorption medium, thus reducing the ability to capture (F^-) anions, thus maintaining their high concentration in the solution, thus reducing the removal rate. Therefore, in light of the current results, 5.5 is the optimal value for removing fluoride anions (F^{-}) from contaminated aqueous solutions using cobalt oxide nanoparticles.

4.2 Effect of agitation speed change on the fluoride anions recovery:

Determining the agitation speed in batch adsorption systems is a vital factor for determining the optimum efficiency of the treatment process. Over the range of 100-500 rpm, the effect of this factor on the recovery efficiency of fluoride ions (F^-) was studied, with other operational parameters held constant at 5.5, 1 ppm, 0.1 g, 180 min, and 25 °C for pH, initial concentration of fluoride anions (F^-) , dosage of cobalt oxide nanoparticle, contact time, and temperature, respectively.

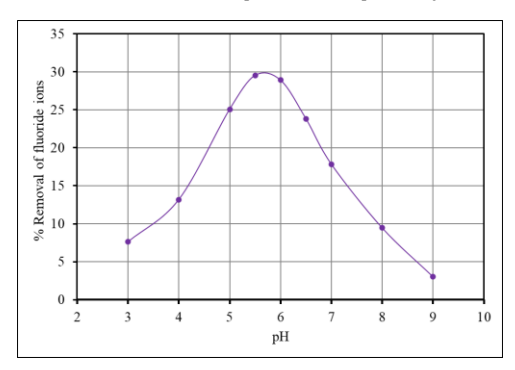


Figure 12: Effect of acid function on the fluoride anions adsorption by nano Co₃O₄

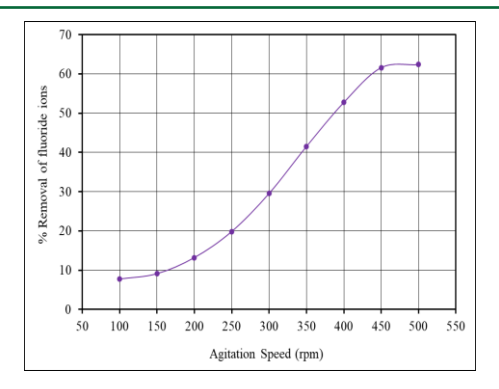


Figure 13: Effect of agitation speed on the fluoride anions adsorption by nano Co₂O₄

Figure 13 represents the experimental results obtained from varying the agitation rate on the removal efficiency of fluoride anions (F^{-}) from the contaminated aqueous solution using cobalt oxide nanoparticles. It is noted that the relationship between the two parameters is a clear direct relationship, as the removal percentage increases from 7.7-62.4% with the increase in the agitation speed from 100-450 rpm, respectively, while the treatment efficiency remains constant without change despite raising the vibration to 500 rpm. This result may be explained by the fact that the distribution of fluoride anions (F^-) was insufficient to migrate to the adsorbent surface at slow and medium agitation speeds. The distribution may also have been insufficient to break down the film formed on the adsorbent surface, as the removal efficiency did not exceed 30% at 300 rpm. However, by increasing the agitation speed to 350 rpm, the treatment efficiency begins to improve and reaches more than 40%, due to the increase in the momentum of solution and the beginning of the decomposition of the film layer that prevents the fluoride anions (F^{-}) from reaching the surface of the cobalt oxide nanoparticles, which contributes to their association with the active groups on the surface of the cobalt oxide nanoparticles. By increasing the agitation speed to 400 and then to $450\ \text{rpm}$, the adsorption efficiency increases due to the increase in the number of adsorbed fluoride anions (F^{-}) for the same reason mentioned above. However, increasing the agitation speed beyond 450 rpm has no significant effect on the treatment process, and the removal percentage remains unchanged. The reason for the lack of efficiency may be that the adsorption capacity of the adsorbent has reached its maximum value and is no longer able to absorb any additional amount of target anions. Alternatively, it is possible that increasing the shaking to very high values increased the friction between the cobalt oxide nanoparticles and the walls of the experimental flask, resulting in physical changes that contributed to the stabilization of adsorption efficiency. Therefore, the results obtained from changing this operating parameter indicate the existence of a specific saturation point, beyond which increasing the speed does not lead to further improvement in the adsorbent performance.

$4.3\ Effect$ of change the initial concentration of fluoride anions on the recovery

Initial concentration is one of the factors associated with the contaminated solution. Determining the initial concentration at which the maximum adsorbed concentration is obtained by the substance contributes to determining the behavior of the adsorbent and its maximum adsorption capacity. The performance of prepared cobalt oxide nanoparticles was tested to treat very high concentrations of fluoride anions (F^-) , up to 25 times the highest concentration permitted worldwide. Keeping the rest operational parameters constant at 5.5, 450 rpm, 0.1 g, 180 min, 25 °C for pH, agitation speed, Co₃O₄ nanoparticles dosage, contact time, temperature, respectively, the effect of this factor on the recovery efficiency of fluoride anions (F^-) was investigated. As shown in Figure 14, the treatment efficiency has an inverse relationship with the initial concentration but at the same time it is directly related to the adsorbed concentration (Cads). At low concentrations, the percentage of fluoride anion removal (F^-) from the solution is at its highest, starting at 62.4% at 1 ppm and gradually decreasing to 13.8% at 100 ppm. Meanwhile, the adsorption capacity increases from 6.24 to 138 mg/g with increasing initial concentration from 1 to 100 ppm, respectively. As is known, the adsorption efficiency is related to the surface area. At low initial concentrations, removal is high because most of the active sites are unoccupied and can capture the pollutant ions with high performance. As the initial concentration increases, the efficiency begins to decrease, because the fixed amount of adsorbent has a specific capacity to absorb the target anions, which makes their residual concentration in the solution high with increasing initial concentration. According to equation (1), the

percentage removal will be low.

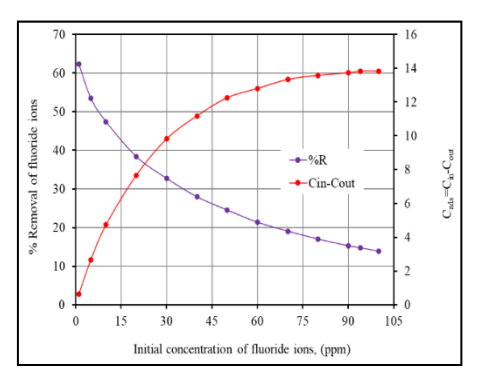


Figure 14: Effect of initial concentration of fluoride anions on adsorption by nano Co₃O₄

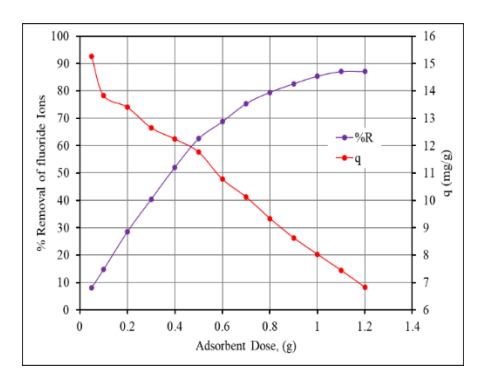


Figure 15: Effect of nano Co₃O₄ dose on the fluoride anions adsorption

While the adsorption capacity has an opposite direction to the removal efficiency according to equation (2), as the adsorbed concentration (Cads) will gradually increase as a result of the active sites being filled with fluoride anions (F^-) , and given the constant dose of the adsorbent, the value of the adsorption capacity will increase with the increase in the initial concentration. It is also noted from Figure 14 that the adsorbed concentration remains constant after 94 ppm at 13.8 ppm, and this is due to two possibilities: the first is that the affinity of the cobalt oxide nanoparticles has reached its maximum value such that they are unable to capture any additional fluoride anions (F^-) . The second possibility is that the concentration of the contaminant in the solution and on the surface of the adsorption medium are in equilibrium, such that the number of anions adsorbed on the surface of the adsorbent equals the number of anions lost from it. According to these results, the prepared cobalt oxide nanoparticles demonstrated excellent adsorbent performance, and the optimum initial concentration of fluoride anions (F^{-}) for treatment is 94 ppm.

$4.4\ Effect$ of change the adsorbent dose on the recovery of fluoride anions

This factor is one of the most important factors determining the economics of a treatment process, regardless of whether the adsorbent is expensive or invaluable. If the adsorption medium requires high manufacturing costs, the required dosage must be precisely determined and utilized optimally. However, if the adsorbent is readily available and nonvaluable material, determining its optimal dosage is of utmost importance. This is because an additional dosage means additional weight for the system to bear, requiring higher manufacturing costs. Furthermore, the material accumulated after the adsorption process is larger, meaning additional costs for safe and environmentally friendly disposal. Figure 15 illustrates the effect of varying the cobalt oxide nanoparticles dosage within the range of 0.05-1.2 g on the removal efficiency of fluoride anions (F^-) from contaminated aqueous solutions, keeping all other operational parameters held constant at 5.5, 450 rpm, 94 ppm, 180 min, and 25 °C for pH, agitation speed, initial fluoride ion concentration (F^-), contact time, and temperature, respectively. It is clear that the adsorption efficiency increases with the increase of the adsorbent dosage, increasing from 8.11 at $0.05\,\mathrm{g}$ to 87.05% at $1.1\,\mathrm{g}$. This result can be explained by a well-known fact: increasing the adsorption dose results in an increase in the number of functional groups and active sites due to an increase in the surface area exposed to adsorption. This contributes to the absorption of a larger number of target anions, thus reducing their concentration in the solution and increasing efficiency. While the adsorption capacity behaves differently, as it decreases with increasing adsorption dose, and since the capacity represents the ratio between the adsorbent concentration and the adsorbent dose, and since the increase in the adsorbent mass is higher than the increase in the adsorbent concentration, then the adsorption capacity will decrease according to equation (2). While after reaching the maximum efficiency at a dose of 1.1 g of the adsorbent, the removal remains constant without change, and the reason for this may be the accumulation of the adsorbent in the experimental flask in a way that does not allow the fluoride anions (F^-) to reach the active sites on the surface of the cobalt oxide nanoparticles. Or the adsorption medium has reached saturation under the specified operating conditions, such that it cannot accept any more contaminant anions. Therefore, the optimal dosage to remove 87% of the 94 ppm of fluoride anions (F^-) is 1.1 g of cobalt oxide nanoparticles.

4.5 Effect of change the contact time on the recovery of fluoride anions

As with the previous variable, determining the appropriate time achieves the economic feasibility of the treatment process, as a short time makes the process inefficient, and a long time makes the process expensive due to energy consumption and increased operating costs. This important factor was studied over a period of 10-200 min, which covers most of the time periods reported in the literature. Other operating conditions were kept constant at 5.5, 450 rpm, 94 ppm, 1.1, and 25 °C for pH, agitation speed, initial fluoride anion concentration (F^{-}) , adsorbent dosage, and temperature, respectively. Figure 16 reveals that the relationship between the change in contact time and the removal of fluoride anions (F^-) from the aqueous solution is a clear direct relationship, where the removal is low at short time periods and vice versa. Increasing the contact time provides sufficient time for the target anions to reach the active sites on the surface of the adsorbent, unlike short time periods. It is noted from Figure 16 that the removal efficiency increased from 8.5% at 10 minutes to reach 41.6% at the end of the first hour, i.e. an increase of five times the initial value. It is noteworthy that the removal percentage in the second hour was close to that in the first hour. After 120 minutes of treatment, the efficiency reached 72%, while in the third hour it increases with only half of what it was, reaching 87%, which is the maximum value at 180 minutes of treatment start. This result can be explained by the fact that the active sites on the surface of the material were not fully occupied and could receive a large number of fluoride anions (F^-) , so the efficiency increased gradually and with almost constant differences.

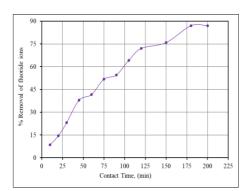


Figure 16: Effect of contact time on the fluoride anions adsorption by nano Co_3O_4

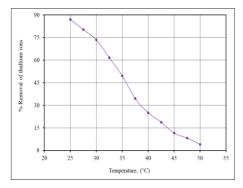


Figure 17: Effect of temperature on the fluoride anions adsorption by nano Co₃O₄

However, beyond 120 minutes, the difference in efficiency began to decline during this time period due to the active sites being filled with adsorbed ions, which created a state of competition between fluoride anions for the same number of active sites, which led to a decrease in the ability to capture ions by half. It is also noted that after an additional 20

minutes had passed over the three hours, there was no change in the removal efficiency, but rather it remained constant. The reason for this is either that the material had actually reached a state of saturation and was no longer able to receive any additional quantity of pollutant. Or it has reached an equilibrium state where the number of ions adsorbed on the adsorption surface equals the number of ions lost from it. Therefore, 180 minutes is considered the optimal time to reach the maximum removal efficiency of negative fluoride ions (F^-) using 1.1 g of cobalt oxide nanoparticles.

4.6 Effect of change the temperature on the recovery of fluoride anions

Temperature significantly affects the adsorption process, as it has a dual effect on both the contaminant and the adsorbent. The effect of temperature on the ability of cobalt oxide nanoparticles to recover fluoride anions (F^{-}) from contaminated aqueous solutions was investigated over a temperature range of 25-50 °C, which represents the general temperature distribution in almost all temperate and hot environments. Experiments for this variable were conducted by keeping the rest operational variables held constant at the optimum values of 5.5, 450 rpm, 94 ppm, 180 min, 1.1 g each for pH, agitation speed, initial concentration of fluoride anions (F^-) , contact time, and adsorbent dose, respectively. The obtained results, shown in Figure 17, indicated that the increase in temperature was accompanied by a continuous dramatic decrease in the adsorption efficiency, reaching approximately 22 times, as it decreased from 87% at 25 °C to 4% at 50 °C. The reason for these decreases is due to several possible factors, the first of which is that increasing temperature may lead to a steady increase in the kinetic energy of the target anions, which reduces their chances of reaching the active sites and adhering to them to achieve the adsorption mechanism. Or the increase in temperature led to providing the energy needed to separate the molecules and weaken the attractive forces between them and the active sites that adsorb them, which prompts the desorption process. It is possible that increasing the temperature leads to changes in the nature of the adsorption surface, such as shrinking the pores or breaking the surface bonds, which leads to a reduction in the capture of fluoride anions (F^-) . In all of the above scenarios, the concentration of target ions in the solution will be high, and thus the adsorption efficiency will be reduced. Therefore, nanoscale cobalt oxide is highly efficient at treating contaminated solutions at low temperatures.

5. CONCLUSIONS

The current study revealed many important conclusions, the most significant of which is the possibility of exploiting wasted tree leaves in preparing materials with an important environmental impact. Cobalt oxide (Co₃O₄) nanoparticles were synthesized using the green method from the aqueous extract of the Iraqi mandarin plant leaves and cobalt nitrate hexahydrate as a precursor, in a simple and economical way. Various morphological tests indicated the success of the synthesis method. The prepared material was within the nanoscale range with an average size of 271.48 nm, had high porosity, a surface area of 329 m²/g, and various active groups. It had magnetic properties and a regular crystalline structure, and its point of zero charge value was 7.88. Experimental tests proved that the prepared nanomaterial had an excellent performance as an adsorption medium in recovering fluoride anions (F^-) from contaminated aqueous solutions with a maximum efficiency of 87% and an adsorption capacity of 7.43 mg/g. The optimum conditions for the treatment process were 1.1 g, 450 rpm, 25 °C, 94 ppm, 5.5, and 180 min for each of the cobalt oxide nanoparticles dosage, agitation speed, temperature, initial fluoride ion (F^-) concentration, pH, and contact time, respectively. The acid function had a dual effect on the removal efficiency, as it was characterized by a direct relationship in acidic environments and an inverse relationship in neutral and almost basic environments. The efficiency increased with increasing agitation speed, adsorbent dose, and contact time, while the other variables had an inverse effect.

FUNDING

This research was entirely self-financed and did not receive any external funding.

CONFLICT OF INTEREST

The authors declare that they have no conflicts of interest to disclose

ACKNOWLEDGMENTS

The authors would like to thank Mustansiriyah University (www.uomustansiriyah.edu.iq), Baghdad – Iraq, and Mutah University (www.mutah.edu.jo/), Al Karak – Jordan, and University of Diyala (https://uodiyala.edu.iq/), Diyala – Iraq, for their support in the present

work.

REFERENCES

- Abbas F.S., Abdulkareem W.S., Abbas M.N. 2022b. Strength Development of Plain Concrete Slabs by the Sustainability Potential of Lead-Loaded Rice Husk (LLRH). Journal of Applied Engineering Science, 20, 1, Pp. 160-167. https://doi:10.5937/jaes0-32253
- Abbas M.N. 2015. Phosphorus removal from wastewater using rice husk and subsequent utilization of the waste residue. Desalination and Water Treatment, 55, 4, Pp. 970-977. https://doi.org/10.1080/19443994.2014.922494
- Abbas M.N., Abbas F.S. 2013a. Iraqi Rice Husk Potency to Eliminate Toxic Metals from Aqueous Solutions and Utilization from Process Residues. Advances in Environmental Biology, 7, 2, Pp. 308-319. https://www.aensiweb.com/old/aeb/2013/308-319.pdf
- Abbas M.N., Abbas F.S. 2013b. The Predisposition of Iraqi Rice Husk to Remove Heavy Metals from Aqueous Solutions and Capitalized from Waste Residue. Research Journal of Applied Sciences, Engineering and Technology, 6, 22, Pp. 4237-4246. https://www.maxwellsci.com/html/rjaset.6.3539.html
- Abbas M.N., Abbas F.S. 2013c. The Feasibility of Rice Husk to Remove Minerals from Water by Adsorption and Avail from Wastes. Research Journal of Applied Sciences, WSEAS Transactions on Environment and Development, 9, 4, Pp. 301-313. http://www.wseas.org/multimedia/journals/environment/2013/145715-140.pdf
- Abbas M.N., Abbas F.S. 2014. Application of Rice Husk to Remove Humic Acid from Aqueous Solutions and Profiting from Waste Leftover. WSEAS Transactions on Biology and Biomedicine, 11, 9, Pp. 62-69. http://www.wseas.us/journal/pdf/biology/2014/a025708-124.pdf
- Abbas M.N., Alalwan H.A. 2019. Catalytic Oxidative and Adsorptive Desulfurization of Heavy Naphtha Fraction. Korean Journal of Chemical Engineering, 12, 2, Pp. 283-288. http://doi.org/10.9713/kcer.2019.57.2.283
- Abbas M.N., Al-Hermizy S.M.M., Abudi Z.N., Ibrahim T.A. 2019a. Phenol Biosorption from Polluted Aqueous Solutions by Ulva lactuca Alga using Batch Mode Unit. Journal of Ecological Engineering, 20, 6, Pp. 225–235. https://doi.org/10.12911/22998993/109460
- Abbas M.N., Ali S.T., Abbas R.S. 2020. Rice Husks as a Biosorbent Agent for Pb+2 Ions from Contaminated Aqueous Solutions: A Review. Biochemical and Cellular Archives, 20, 1, Pp. 1813-1820. https://doi.org/10.35124/bca.2020.20.1.1813
- Abbas M.N., Al-Madhhachi A.T., Esmael S.A. 2019b. Quantifying soil erodibility parameters due to wastewater chemicals. International Journal of Hydrology Science and Technology, 9, 5, Pp. 550-568. http://doi.org/10.1504/IJHST.2019.10016884
- Abbas M.N., Al-Tameemi I.M., Hasan M.B., Al-Madhhachi A.T. 2021. Chemical Removal of Cobalt and Lithium in Contaminated Soils using Promoted White Eggshells with Different Catalysts. South African Journal of Chemical Engineering, 35, Pp. 23-32. https://doi.org/10.1016/j.sajce.2020.11.002
- Abbas M.N., Ibrahim S.A. 2020. Catalytic and thermal desulfurization of light naphtha fraction. Journal of King Saud University Engineering Sciences, 32, 4, Pp. 229-235. https://doi.org/10.1016/j.jksues.2019.08.001
- Abbas M.N., Ibrahim S.A., Abbas Z.N., Ibrahim T.A. 2022a. Eggshells as a Sustainable Source for Acetone Production. Journal of King Saud University Engineering Sciences, 34, 6, Pp. 381-387. https://doi.org/10.1016/j.jksues.2021.01.005
- Abbas M.N., Nussrat T.H. 2020. A statistical analysis of experimental data for the adsorption process of cadmium by watermelon rinds in a continuous packed bed column. International Journal of Innovation, Creativity and Change, 13, 3, Pp. 124-138. https://www.ijicc.net/images/vol_13/Iss_3/13321_Abbas_2020_E_R.pdf
- Abd ali I.K., Ibrahim T.A., Farhan A.D., Abbas M.N. 2018. Study of the effect of pesticide 2,4-D on the histological structure of the lungs in the albino mice (Mus musculus). Journal of Pharmaceutical Sciences and Research, 10, 6, Pp. 1418-1421. https://www.jpsr. pharmainfo.in/Documents/Volumes/vol10Issue06/jpsr10061822.p
- Abd Ali I.K., Salman S.D., Ibrahim T.A., Abbas M.N. 2024. Study of the

- Teratogenic Effects of Antimony on Liver in the Adult Rabbit (Oryctolagus cuniculus). Advancements in Life Sciences, 11, 2, Pp. 462-469. http://dx.doi.org/10.62940/als.v11i2.2773
- Abd Al-Latif F.S., Ibrahim T.A., Abbas M.N. 2023. Revealing Potential Histological Changes of Deltamethrin Exposure on Testicular Tissue in Albino Rabbits (Oryctolagus cuniculus). Advancements in Life Sciences, 10, 4, Pp. 619-626. http://dx.doi.org/10.62940/als. v10i4 2323
- Abdulkareem W.S., Aljumaily H.S.M., Mushatat H.A., Abbas M.N. 2023. Management of Agro-Waste by Using as an Additive to Concrete and Its Role in Reducing Cost Production: Impact of Compressive Strength as a Case Study. International Journal on "Technical and Physical Problems of Engineering" (IJTPE), 15, 1, Pp. 62-67.
- Abdullah W.R., Alhamadani Y.A.J., Abass I.K., Abbas M.N. 2023. Study of chemical and physical parameters affected on purification of water from inorganic contaminants. Periodicals of Engineering and Natural Sciences, 11, 2, Pp. 166-175. http://dx.doi.org/10.21533/pen.v11i2.3508
- Ahmad S., Singh R., Arfin T., Neeti K., 2022. Fluoride contamination, consequences and removal techniques in water: a review. Environmental Science: Advances, 1. https://doi.org/10.1039/d1va00039j
- Al-Ali S.I.S., Abudi Z.N., Abbas M.N. 2023. Modelling and Simulation for the use of Natural Waste to Purified Contaminated Heavy Metals. Journal of the Nigerian Society of Physical Sciences, 5, 1, 1143. https://doi.org/10.46481/jnsps.2023.1143
- Alalwan H.A., Abbas M.N., Abudi Z.N., Alminshid A.H. 2018. Adsorption of thallium ion (Tl+3) from aqueous solutions by rice husk in a fixed-bed column: Experiment and prediction of breakthrough curves. Environmental Technology and Innovation, 12, Pp. 1-13. https://doi.org/10.1016/j.eti.2018.07.001
- Alalwan H.A., Abbas M.N., Alminshid A.H. 2020. Uptake of Cyanide Compounds from Aqueous Solutions by Lemon Peel with Utilising the Residue Absorbents as Rodenticide. Indian Chemical Engineer, 62, 1, Pp. 40-51. https://doi.org/10.1080/00194506.2019.162 3091
- Alalwan H.A., Mohammed M.M., Sultan A.J., Abbas M.N., Ibrahim T.A., Aljaafari H.A.S., Alminshid A.A. 2021. Adsorption of methyl green stain from aqueous solutions using non-conventional adsorbent media: Isothermal kinetic and thermodynamic studies. Bioresource Technology Reports, 14, 100680. https://doi.org/10.1016/j.biteb.2021.100680
- Alhamd S.J., Abbas M.N., Al-Fatlawy H.J.J., Ibrahim T.A., Abbas Z.N. 2024a. Removal of phenol from oilfield produced water using non-conventional adsorbent medium by an eco-friendly approach. Karbala International Journal of Modern Science (KIJOMS), 10, 2, Pp. 191-210. https://doi.org/10.33640/2405-609X.3350
- Alhamd S.J., Abbas M.N., Manteghian M., Ibrahim T.A., Jarmondi K.D.S. 2024b. Treatment of Oil Refinery Wastewater Polluted by Heavy Metal Ions via Adsorption Technique using Non-Valuable Media: Cadmium Ions and Buckthorn Leaves as a Study Case. Karbala International Journal of Modern Science (KIJOMS), 10, 1, Pp. 1-18. https://doi.org/10.33640/2405-609X.3334
- Alhamd S.J.K., Manteghian M., Abdulhameed M.A., Ibrahim T.A., Jarmondi K.D.S. 2024c. Efficient Removal of Heavy Metals from Crude Oil Using High Surface Area Adsorbent Media: Vanadium as a Case Study. Tikrit Journal of Engineering Sciences (TJES), 10, 1, Pp. 1-9. https://doi.org/10.25130/tjes.31.2.1
- Al-Hermizy S.M.M., Al-Ali S.I.S., Abdulwahab I.A., Abbas M.N. 2022. Elimination of Zinc Ions (Zn+2) from Synthetic Wastewater Using Lemon Peels. Asian Journal of Water, Environment and Pollution, 19, 5, Pp. 79-85. https://doi.org/10.3233/AJW220073
- Al-Hermizy S.M.M., Awadh H.A., Abbas M.N. 2025. Biosorption technique using water hyacinth plant as an effective and sustainable approach for treating oil refinery waste: Vanadium element as a case study, Journal of Ecological Engineering, 26, 6, 251-272. https://doi.org/10.12911/22998993/202658
- Ali G.A.A., Abbas M.N. 2020. Atomic Spectroscopy Technique Employed to Detect the Heavy Metals from Iraqi Waterbodies Using Natural Bio-Filter (Eichhornia crassipes) Thera Dejla as a Case Study. Systematic Reviews in Pharmacy, 11, 9, Pp. 264-271. https://doi.org/10.31838/srp.2020.9.43

- Ali G.A.A., Ibrahim S.A., Abbas M.N. 2021. Catalytic Adsorptive of Nickel Metal from Iraqi Crude Oil using non-Conventional Catalysts. Innovative Infrastructure Solutions, 6, 7, Pp. 1-9. https://doi.org/10.1007/s41062-020-00368-x
- Ali S.A.K., Abudi Z.N., Abbas M.N., Alsaffar M.A., Ibrahim T.A. 2024a. Synthesis of Nano-silica Particles using Eucalyptus globulus Leaf Extract and Their Innovative Application as an Adsorbent for Malachite Green Dye. Russian Journal of Applied Chemistry, 97, 1, Pp. 2–14. https://doi.org/10.1134/S1070427224010099
- Ali S.A.K., AL-Kaabi Z., Kasim M.N., Abbas M.N., Ibrahim T.A. 2023. Remediation of Antimony from Aqueous Solutions by Adsorption Technique: Isothermal, Kinetic and Thermodynamic Studies. Indian Journal of Environmental Protection, 43, 14, Pp. 1316-1325, (Conference 2023). https://www.e-ijep.co.in/43-14-1316-1325/
- Ali S.A.K., Almhana N.M., Hussein A.A., Abbas M.N. 2020a. Purification of Aqueous Solutions from Toxic Metals using Laboratory Batch Mode Adsorption Unit: Antimony (V) Ions as a Case Study. Journal of Green Engineering (JGE), 10, 11, 10662-10680.
- Ali S.T., Qadir H.T., Moufak S.K., Al-Badri M.A.M., Abbas M.N. 2020b. A Statistical Study to Determine the Factors of Vitamin D Deficiency in Men: The City of Baghdad as a Model. Indian Journal of Forensic Medicine and Toxicology, 14, 1, Pp. 691-696. https://doi.org/10.37506/ijfmt.v14i1.132
- Ali S.T., Shahadha R.W., Abdulkareem W.S., Abbas M.N. 2024b. Available Low Cost Agro-Waste as an Efficient Medium to Eliminate Heavy Metal Contamination using Sustainable Approach Achieving Zero Residue Level. Journal of Ecological Engineering, 25, 10, Pp. 160-175. https://doi.org/10.12911/22998993/191945
- Alminshid A.H., Abbas M.N., Alalwan H.A., Sultan A.J., Kadhome M.A. 2021.
 Aldol condensation reaction of acetone on MgO nanoparticles surface:
 An in-situ drift investigation. Molecular Catalysis, 501, 111333.
 https://doi.org/10.1016/j.mcat. 2020. 111333
- Alminshid A.H., Alalwan H.A., Mohammed M.M., Abbas M.N. 2025. Spectroscopic study of methane reaction mechanism on MgO nanoparticles. Ionic, 31, Pp. 3861–3866. https://doi.org/10.1080/00194506.2025.2459833
- Alsarayreh A. A., Nsaif R.Z., Nsaif M.M., Nsaif Z.M., Abbas M.N. 2025a. Nickel Remediation by Adsorption Technique Achieving the Concept of Zero Residue Level. The Jordan Journal of Civil Engineering (JJCE), 19, 1, Pp. 13-29. https://doi.org/10.14525/JJCE. v19i1.02
- Alsarayreh A.A., Al-zoubi H.Q., Abbas M.N. 2025b. Sustainable nickel removal from water by using waste tea leaves for eco-friendly water treatment. Indian Chemical Engineer, 1-22. https://doi.org/10.1080/00194506.2025.2459833
- Alsarayreh A.A., Ibrahim S.A., Alhamd S.J., Ibrahim T.A., Abbas M.N. 2024. Removal of selenium ions from contaminated aqueous solutions by adsorption using lemon peels as a non-conventional medium. Karbala International Journal of Modern Science (KIJOMS), 10, 4, Pp. 511–531. https://doi.org/10.33640/2405-609X.3375
- Alwan E.K., Hammoudi A.M., Abd I.K., Abd Alaa M.O., Abbas M.N. 2021. Synthesis of Cobalt Iron Oxide Doped by Chromium Using Sol-Gel Method and Application to Remove Malachite Green Dye. NeuroQuantology, 19, 8, Pp. 32-41 http://doi:10. 14704/nq.2021.19.8.NQ21110
- Everett E. T. 2011. Fluoride's effects on the formation of teeth and bones, and the influence of genetics. Journal of dental research, 90, 5, Pp. 552–560. https://doi.org/10.1177/002 2034510384626
- Gadooa Z.A., Alsarayreh A.A., Abbas M.N. 2025. Adsorption of thallium using tangerine peels and exploitation from the waste in an ecofriendly manner. Ecological Engineering and Environmental Technology, 26, 2, Pp. 131-152, https://doi.org/10.12912/27197050/ 196880
- Ghulam N.A., Abbas M.N., Sachit D.E. 2020. Preparation of synthetic alumina from aluminium foil waste and investigation of its performance in the removal of RG-19 dye from its aqueous solution. Indian Chemical Engineer, 62, 3, Pp. 301–313. https://doi.org/10.1080/00194506.2019.1677512
- Guth S., Hüser S., Roth A., Degen G., Diel P., Edlund K., Eisenbrand G., Engel K.H., Epe B., Grune T., Heinz, V., Henle T., Humpf H.U., Jäger H., Joost H.G., Kulling S.E., Lampen A., Mally A., Marchan R., Marko D., Hengstler J.G. 2020. Toxicity of fluoride: critical evaluation of evidence for human

- developmental neurotoxicity in epidemiological studies, animal experiments and in vitro analyses. Archives of toxicology, 94, 5, Pp. 1375–1415. https://doi.org/10.1007/s00204-020-02725-2
- Hamdi G.M., Abbas M.N., Ali S.A.K. 2024. Bioethanol Production from Agricultural Waste: A Review. Journal of Engineering and Sustainable Development, 28, 2, Pp. 233–252. https://doi.org/10.31272/jeasd.28.2.7
- Hameed W.A., Abbas M.N. 2024. Dyes Adsorption from Contaminated Aqueous Solution Using SiO2 Nanoparticles Prepared from Extracted Tree Leaves. Journal of Ecological Engineering, 25, 7, Pp. 41-57. https://doi.org/10.12911/22998993/187921
- Hammed A.S., Alsarayreh A.A., Abbas M.N. 2025. Applying of zero residue level concept in integrated management of toxic and solid wastes as a sustainable approach. Ecological Engineering and Environmental Technology, 25, 1, Pp. 353–378. https://doi.org/10. 129 12/27197050/196409
- Hasan M.B., Al-Tameemi I.M., Abbas M.N. 2021. Orange Peels as a Sustainable Material for Treating Water Polluted with Antimony. Journal of Ecological Engineering, 22, 2, Pp. 25-35. https://doi.org/10.12911/22998993/130632
- Hashem N.S., Ali G.A.A., Jameel H.T., Khurshid A.N., Abbas M.N. 2021. Heavy Metals Evaluation by Atomic Spectroscopy for Different Parts of Water Hyacinth (Eichhornia Crassipes) Plants: Banks of Tigris River and Al-Zuhairat Village Sites. Biochemical and Cellular Archives, 21, 2, Pp. 3813-3819. https://connectjournals.com/03896.2021.21.3813
- Ibrahim S.A., Alhamd S.J.K., Ali S.M., Abbas M.N., Ibrahim T.A., Alsarayreh A.A. 2025. Remediation of aqueous solutions contaminated by benzidine toxic dye using non-conventional adsorbent: morphological and modelling studies, Al-Qadisiyah Journal for Engineering Sciences (QJES), 18(2), Pp. 066-078. https://doi.org/10.30772/qjes.2024. 149956.1244
- Ibrahim S.A., Hasan M.B., Al-Tameemi I.M., Ibrahim T.A., Abbas M.N. 2021. Optimization of adsorption unit parameter of hardness remediation from wastewater using low-cost media. Innovative Infrastructure Solutions, 6, 4, Article number: 200. https://doi.org/ 10.1007/s41062-021-00564-3
- Ibrahim T.A., Mahdi H.S., Abbas R.S., Abbas, M.N. 2020b. Study the Effect of Ribavirin Drug on the histological structure of the testes in Albino mice (Mus musculus). Journal of Global Pharma Technology, 12, 02 Suppl., Pp. 142-146. http://www.jgpt.co.in/ index.php/jgpt/article/view/3233
- Ibrahim T.A., Mohammed A.M., Abd ali I.K., Abbas M.N., Hussien S.A. 2020a. Teratogenic Effect of Carbamazepine Drug on the Histological Structure of Testes in the Albino Mouse (Mus musculus). Indian Journal of Forensic Medicine and Toxicology, 14, 4, Pp. 1829-1834. https://doi.org/10.37506/ijfmt.v14i4.11809

- Iraqi drinking water quality specifications standard IQS/417, ICS :13.060.20,2001
- Jaudenes J.R., Gutiérrez Á.J., Paz S., Rubio C., Hardisson A. 2020. Fluoride Risk Assessment from Consumption of Different Foods Commercialized in a European Region. Applied Sciences, 10, 18, 6582. https://doi.org/10.3390/app10186582
- Karunanithi M., Agrawal R., Qanungo K. 2023. A Review of Fluoride Removal from Ground Water by Various Adsorption Techniques. Journal of the Chilean Chemical Society, 68, 2, Pp. 5839–5846. https://doi.org/10.4067/s0717-97072023000205839
- Khaleel L.R., Al-Hermizy, S.M., Abbas, M.N. 2022. Statistical Indicators for Evaluating the Effect of Heavy Metals on Samaraa Drug Industry Water Exposed to the Sun and Freezing. Tropical Journal of Natural Product Research, 6, 12, Pp. 1969-1974. http://www. doi.org/ 10.26538/tjnpr/v6i12.12
- Khudair S.Y., Alsarayreh, A.A., Abbas M.N. 2024. Adsorption of Vanadium from Iraqi Crude Oil on Nano Zeolite and Alum Sludge. Journal of Engineering and Sustainable Development (JESD), 28, 6, Pp. 762-769. https://doi.org/10.31272/jeasd.28.6.9
- Maddodi S.A., Alalwan H.A., Alminshid A.H., Abbas M.N. 2020. Isotherm and computational fluid dynamics analysis of nickel ion adsorption from aqueous solution using activated carbon. South African Journal of Chemical Engineering, 32, Pp. 5-12. https://doi.org/10.1016/j.sajce.2020.01.002
- National Center for Biotechnology Information (NCBI). 2025. PubChem Compound Summary for CID 28179, Fluoride Ion. Retrieved April 24, 2025 from https://pubchem.ncbi.nlm.nih.gov/compound/Fluoride-Ion
- Rajaa N., Kadhim F.J., Abbas M.N., Banyhussan Q.S., 2023. The improvement of concrete strength through the addition of sustainable materials (agro-waste loaded with copper ions). 3rd International Conference for Civil Engineering Science (ICCES 2023), IOP Conf. Series: Earth and Environmental Science, 1232, 012038, 9 Pages. http://doi.org/10.1088/1755-1315/1232/1/012038
- Shadhan Z.J., Alhamd S., Abbas M.N. 2024. Recovery of vanadium element from wastewater of petroleum refineries using effective adsorbent: Mathematical approach via isothermal, kinetics and thermodynamic simulation. Al-Qadisiyah Journal for Engineering Sciences (QJES), 17, 3, Pp. 211-219. https://doi.org/10.30772/qjes.2024.145441.1069
- Shaji E., Sarath K.V., Santosh M., Krishna Prasad P.K., Arya B.K., Babu M.S. 2024. Fluoride contamination in groundwater: A global review of the status, processes, challenges, and remedial measures. Geoscience Frontiers, 15, 2, 101734. https://doi.org/ 10.1016/j.gsf.20 23.101734

